Polarization Radar Estimates of Raindrop Size Spectra and Rainfall Rates

A. J. ILLINGWORTH AND I. J. CAYLOR

Department of Pure and Applied Physics, University of Manchester Institute of Science and Technology, Manchester, U.K.

(Manuscript received 18 September 1988, in final form 2 April 1989)

ABSTRACT

The differential reflectivity (Z_{DR}) measures the mean shape of hydrometeors and provides an estimate of the mean size of raindrops. Observations of Z_{DR} for rain may be combined with the conventional radar reflectivity factor (Z) and fitted to any two-parameter raindrop size distribution and this information used to derive more accurate rainfall rates. In such work the precise shape of raindrops is a critical parameter. Recently available data suggest that large raindrops are more oblate than previously believed. These new shapes support the idea that Z_{DR} values above 3.5 dB can be attributed to rain. Average values of Z_{DR} as a function of Z obtained in heavy rain by the Chilbolton radar agree very closely with those predicted using the new shapes. Statistics are also presented of the natural variability of raindrop spectra in heavy rain. Analytic expressions are proposed for computing rainfall rate from Z and Z_{DR}.

1. Introduction

The radar reflectivity factor, Z, of rain measured by a conventional radar is not a unique function of the rainfall rate or the mean size of the raindrops, but is given by the product ND^6, where N is the concentration of drops of diameter D, summed over all the drop sizes present. Many different empirical relationships have been proposed relating the rainfall rate (R) to the radar reflectivity (Z). The use of one of these formulae is essentially equivalent to assuming a constant raindrop size distribution. Such relationships reflect an average long term dependence, but the actual rainfall predicted by an individual value of Z is typically in error by a factor of two because of natural fluctuations in the raindrop size spectra (Wilson and Brandes 1979).

Polarization diversity radar provides a second observable parameter, the differential reflectivity, which is related to the mean drop size. When this information is used in conjunction with Z, more accurate rainfall rates may be derived. The differential reflectivity (Z_{DR}) is defined as

$$Z_{DR} = 10 \log(Z_H/Z_V) \quad (1)$$

where Z_H and Z_V are the radar reflectivity factors measured at horizontal and vertical polarizations, respectively. For spherical particles, such as small raindrops, Z_H and Z_V are equal, and Z_{DR} is zero. Larger raindrops are oblate to a degree which depends upon their size, so Z_H exceeds Z_V; Z_{DR} is positive, and its magnitude is related to the mean raindrop size present.

Corresponding author address: Dr. Anthony Illingworth, UMIST, P.O. Box 88, Dept. of Pure and Applied Physics, University of Manchester Institute of Science and Technology, Manchester M60 1QD, England.

When observations of both Z and Z_{DR} are available, then the data can be fitted to any two-parameter raindrop size distribution. Raindrop size distributions are commonly of the exponential form:

$$N(D) = N_0 \exp(-3.67D/D_0) \quad (2)$$

where D is the equivolumetric raindrop diameter of the oblate drops and D_0 is the volume–median drop diameter. Marshall and Palmer (1948) reported that D_0 is a function of rainfall rate and that, on the average, N_0 is 8000 m^{-3} mm^{-1}. Seliga and Bringi (1976) proposed that the value of D_0 may be derived from the magnitude of Z_{DR}, and N_0 may then be found if Z is known.

The differential reflectivity technique relies on a precise knowledge of the shapes of different sizes of raindrops. The Chilbolton radar (Cherry and Goddard 1982) can measure Z_{DR} to an accuracy of about 0.1 dB which is equivalent to a change in raindrop axial ratio of about 0.01. Most Z_{DR} measurements have been interpreted using the laboratory based equilibrium raindrop shapes of Pruppacher and Pitter (1971), who quote errors of about ±0.03 for the axial ratios of the drops up to 4 mm diameter.

In a series of comparisons of Chilbolton radar data with a ground-based disdrometer (Goddard and Cherry 1984; and Goddard et al. 1983), significantly improved agreement between the radar- and disdrometer-derived rainfall rates was obtained if the drops below 3 mm in size were made slightly more spherical than the shapes of Pruppacher and Pitter. The proposed changes in drop shapes were within the experimental error of the Pruppacher and Pitter laboratory measurements; for example, the axial ratio of a 1 mm drop was changed from 0.98 to 1.00. Recently, more accurate measure-

ments of the shape of naturally occurring raindrops using airborne shadowgraph instruments (Chandrasekar et al. 1988) have confirmed that the shapes inferred from the radar are correct and that the smaller drops are indeed slightly more spherical than suggested by Pruppacher and Pitter. New laboratory experiments (Beard and Ochs 1988) on 1.2 and 1.3 mm drops also support this conclusion.

In this paper we direct attention to heavier rainfall with values of Z above 40 dBZ and rainfall rates generally above 10 mm h^{-1}. The precise shapes of raindrops larger than 4 mm are uncertain, but are important for Z_{DR} measurements in heavier rain. Doviak and Zrnić (1984) state that the maximum value of Z_{DR} due to rain should be 3.5 dB. This assertion is based upon Green's (1975) formula for the axial ratio of raindrops, which is very close to the measurements of Pruppacher and Pitter. Using these shapes a 6 mm drop would be associated with a Z_{DR} of 3.8 dB and an 8 mm drop 4.7 dB; summing the weighted contribution of the various drops in a Marshall–Palmer raindrop size distribution leads to the conclusion that the Z_{DR} of rain cannot exceed 3.5 dB. Doviak and Zrnić (1984) suggest that higher values of Z_{DR} result from a measurement related problem or are due to targets other than raindrops and suggest they arise from ice particles which have very oblate shapes when they melt.

Values of Z_{DR} above 3.5 dB and as high as 6 dB have been reported in convective showers (Illingworth et al. 1987) and in view of the above argument it seems logical to attribute such observations to melting ice particles. On closer examination other possibilites arise. Based on a statistical analysis of the high values of Z_{DR} accompanying intense echoes at altitudes where rain is to be expected, Caylor and Illingworth (1986) hypothesized that raindrops larger than 4 mm are more oblate than predicted by Pruppacher and Pitter. This suggestion was prompted by two findings. First, laboratory measurements (Rasmussen et al. 1984) indicate that unless the ice particles are initially extremely oblate, the shapes during melting are no more distorted than those of the same sized water drop. Second, a limited series of aircraft measurements of large drops (Cooper et al. 1983) implied more oblate forms. Beard and Chuang (1987) have recently published more accurate computations of the shape of large drops and in section 2 of this paper we use these new shapes to calculate the values of Z_{DR} to be expected for various raindrop size distributions. The predicted variation of the average values of Z_{DR} as a function of Z using these new shapes is compared with the actual average values observed with the Chilbolton radar. The variation in the naturally occurring spectra around these mean values is discussed in section 3. The implications of these results for rainfall measurement are explored in section 4.

2. The differential reflectivity of heavy rain

a. Drop shapes and differential reflectivity

The axial ratios for drops above 4 mm proposed by Pruppacher and Pitter (1971) are compared with the more recent values obtained by Beard and Chuang (1987) in Table 1. The values of Pruppacher and Pitter have considerable scatter when experimental errors are considered, with, for example, drops between 7 and 8 mm having ratios in the range 0.51–0.69. The uncertainties in axial ratios quoted for Beard and Chuang's model are less than 0.015. For raindrops larger than 2 mm, Beard and Chuang found that the axial ratio is a nearly linear function of size with a fall in axial ratio of about 0.06 for every millimeter increase in size. The 9 mm drop shape entry in Table 1 is taken from the graph in their paper and is consistent with the shape measured by Pruppacher and Beard (1970) in the low turbulence UCLA wind tunnel. The axial ratio for a 10 mm diameter drop is derived by extrapolation of the linear relationship and is not supported by direct evidence.

TABLE 1. Values of axial ratio and Z_{DR} for various sizes of raindrop assuming oblate spheroid shape. The Mie–Gans calculations are supplied by Dr. Holt, Department of Mathematics, University of Essex, and apply to raindrops at 3.0765 GHz. PP shapes refer to Pruppacher and Pitter (1971), BC to Beard and Chuang (1987).

	PP shapes		BC shapes				
					Z_{DR} (dB) (Mie–Gans)		
Size	Axial ratio	Z_{DR} (dB) (Rayleigh–Gans)	Axial ratio	Z_{DR} (dB) (Rayleigh–Gans)	−10°C	0°C	+10°C
4	0.762	2.69	0.778	2.49	—	—	—
5	0.701	3.51	0.708	3.41	3.50	3.48	—
6	0.655	4.16	0.642	4.35	—	4.42	—
7	0.621	4.67	0.581	5.31	—	5.33	—
8	0.583	5.27	0.521	6.34	7.22	6.70	—
9	—		0.46	7.49	—	10.87	10.10
10	—		0.4	8.78	14.15	16.34	18.27

Table 1 shows the different predicted magnitudes of Z_{DR} for the two sets of drop shapes using the simple Rayleigh–Gans theory. This is strictly only applicable to the small drops, and the Mie–Gans theory should be used when the drop diameter becomes a reasonable fraction of the radar wavelength. Beard (1976) found that changes in pressure and temperature have a negligible effect on raindrop shape over all reasonable values to be found in the atmosphere. The values of Z_{DR} using the exact theory are only slightly higher than for Rayleigh scattering apart from drops above 8 mm where the divergence is considerable. Similarly, we note that temperature effects on scattering for a given drop shape are negligible for drops smaller than 8 mm.

Rasmussen et al. (1985) report laboratory experiments of drop shapes in the presence of a vertical electric field. Appreciable changes in axial ratio occurred only for a field above 200 kV m^{-1} and drops larger than 4 mm diameter; the measurements did not encompass drops larger than 5 mm or field orientations other than the vertical. It is generally believed that the field required to trigger lightning in the atmosphere is about 300 kV m^{-1}; regions where the field exceeds 200 kV m^{-1} are likely to be localized in both time and space, and are also more likely to occur where the hydrometeors are in the ice phase. The effects of electric fields on Z_{DR} are likely to be small. If the lightning does occur in a region with large raindrops, however, a localized sudden change in Z_{DR} might occur. Such a step change in Z_{DR} might be detected if the radar was not scanning but was dwelling on the lower regions of an active storm. In view of the changing sensitivity of differently sized large raindrops to field changes apparent in the results of Rasmussen et al. (1985), a quantitative interpretation of any such Z_{DR} jumps will probably not be possible.

b. *Statistical analysis of radar data*

A simple prediction of the values of Z_{DR} to be expected in rain is displayed in Fig. 1 for a Marshall–Palmer raindrop size distribution with a value of N_0 of 8000 m^{-3} mm^{-1}. The two curves are obtained using the two drop shape models in Table 1 for different values of D_0 in Eq. (2) at 0°C and terminating the raindrop spectrum at 8 mm. The curves diverge for values of Z above 40 dBZ; the Pruppacher and Pitter shapes lead to a maximum predicted value of 3.5 dB, whereas the more oblate shapes suggest values of up to 4.5 dB are possible.

The crosses in Fig. 1 represent the average values of Z_{DR} for each 2 dBZ step in Z, obtained from measurements in rain made with the Chilbolton radar during summer convective storms on many different days. Isolated echoes smaller than 2 km in diameter were not included in the analysis. During the observation period, the freezing level was at 3 km or slightly above, and so, to minimize ambiguities due to melting ice particles, data were only analyzed for altitudes below 1 km.

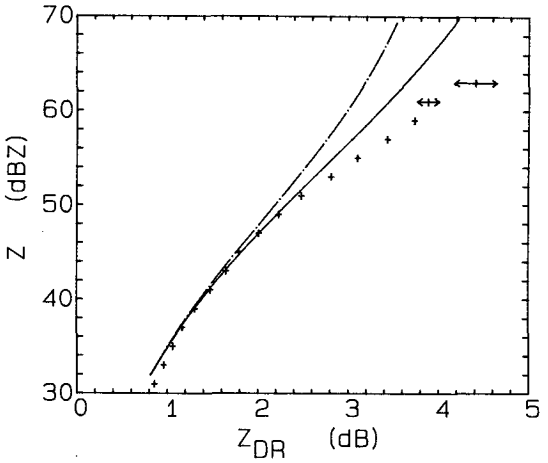

FIG. 1. The variation of Z with Z_{DR} for an exponential drop size distribution using two drop shape models. The solid line is for the Beard and Chuang (1987) drop shapes, and the dashed-dot line is for the Pruppacher and Pitter (1971) shapes. In both cases D_{max} = 8 mm and N_0 = 8000 m^{-3} mm^{-1}. The crosses are averaged Chilbolton radar data collected from summer convective clouds.

It is well established that in severe storms with intense reflectivities, values of Z_{DR} close to zero can extend down to the ground; these signatures are interpreted as hail reaching the ground (e.g., Illingworth et al. 1986). These features are usually quite localized and easy to identify, and so any cell having values at 1 km altitude where Z_{DR} was below 1 dB with Z above 40 dBZ was excluded from the analysis. An example of the average values of Z_{DR} for every 2 dBZ step in Z for such a cell is shown in Fig. 2, where the effect of the hail in reducing the mean values of Z_{DR} for values of Z above 55 dBZ is quite dramatic.

The Z_{DR} values for the averaged data in Fig. 1 are higher than expected and it has been argued that values of Z_{DR} above 3.5 dB should be attributed to raindrops containing melting ice cores (e.g., Doviak and Zrnić 1984; Beard and Chuang 1987). The evidence from the Chilbolton radar does not support this view. Values of Z_{DR} of up to 9 dB have been observed in the bright-band and are thought to result from melting snowflakes and ice crystals, but these only occur in stratiform clouds with a clearly defined melting layer. In vigorous convective storms our observations of many vertical profiles of Z and Z_{DR} indicate that, as ice particles melt, the value of Z_{DR} gradually increases from the zero value associated with graupel and hail, and reaches a maximum value reflecting the equilibrium shape of the raindrop when melting is complete. A typical profile is shown in Fig. 3. The Z_{DR} profiles in convective clouds do not show a maximum associated with the final stages of melting followed by a collapse to a less oblate raindrop containing no ice. Laboratory studies of the melting of ice support this suggestion; Rasmussen et al.

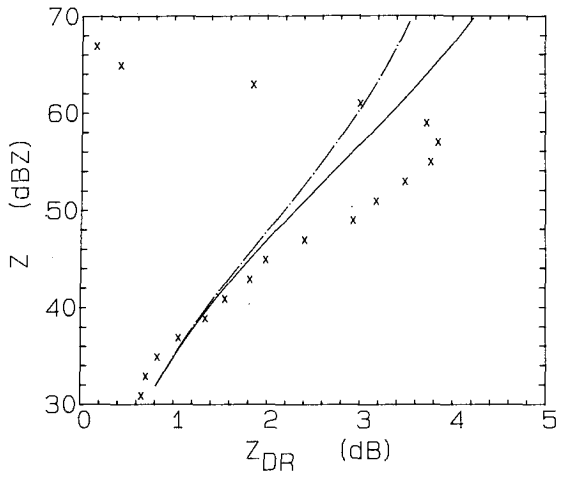

FIG. 2. An example of the effect due to hail showing the significant decrease in Z_{DR} at high Z values. × represents the averaged Chilbolton data from two PPIs through a storm on 6 July 1983, where a hail shaft was identified. The two lines are theoretical Z–Z_{DR} relationships and are identical to those in Fig. 1.

(1984) show that ice spheres smaller than 9 mm do not shed water, but that as melting proceeds they become progressively more oblate, finally assuming the shape of the equivalent diameter water drop. For spheres larger than 9 mm diameter, Rasmussen et al. observed that an unstable torus of liquid water built up around the equator. These ice spheres were tethered within a wind tunnel, but a particle falling in the free atmosphere would be able to tumble and would undoubtedly shed such a torus.

Reflectivity data below 250 m altitude were also excluded from the analysis in Fig. 1, as ground clutter was likely to affect them. Even with this height restriction the quarter degree beamwidth Chilbolton radar still detected the occasional ground return, but the Z_{DR} of such returns is easy to recognize, as the values of Z_{DR} lie in the range +5 to −5 dB and change by several dB between one 300 m long gate and the next (Hall et al. 1984). To suppress this clutter, a Z_{DR} reading was rejected if the change in Z_{DR} (dB) at a neighboring gate was more than 60%.

The average values of Z_{DR} obtained, after the removal of ground clutter and ambiguities due to melting ice, are those displayed in Fig. 1. These data, together with the sample size and standard deviations are summarized in Table 2. If we assume a normal distribution then the standard errors in the mean are only significant for the values of Z in the two highest ranges; these error bars are plotted in the figure.

The use of the Beard and Chuang shapes improves the agreement between the model and the measurements, and we shall use these shapes from now on. The errors in axial ratio of 0.015 are equivalent to a change in Z_{DR} for the raindrops of 0.2 dB, which is still larger than the estimated error of 0.1 dB in the Z_{DR} measurement made by the Chilbolton radar.

c. *Analytic forms of the raindrop spectrum*

We have few direct observations of the concentration of the largest raindrops. The ground-based disdrometer described by Joss and Waldvogel (1967) is widely used for radar validation experiments, but the largest drop size that can be recorded is 5.3 mm; even if the size range was increased, a negligible number of these larger drops would be detected because of the small sample area of the instrument. The data displayed in Fig. 1 were obtained for storms within 100 km range of the Chilbolton radar, but the number of such storms that would be above a single immobile ground-based disdrometer would be extremely small. This restriction does not apply to airborne instruments, and Willis (1984) reports raindrop spectra measured inside a hurricane where the rain rate was computed to be 169 mm h^{-1}, but unfortunately no data are presented for drops greater than 4 mm. This device sampled 2 m^3 of cloud every 10 secs (1.3 km of the flight track); in the heaviest rain it sampled about 20 raindrops in the 4 to 5 mm size range; extrapolating the exponential distribution indicates that such a device would not obtain a significant sample of 8 mm drops. Recently, Beard et al. (1986) have reported finding large raindrops within warm shallow clouds over Hawaii. On one occasion the drop diameter reached 8 mm and the average concentration of raindrops in the 5–6 mm range for the observations was about one per cubic meter. It seems that earlier suggestions that collision induced breakup would limit the maximum raindrop size to a few millimeters have been overemphasized.

Although it appears that large raindrops may well be found in heavy rain, and that such large raindrops would affect the values of Z and Z_{DR}, it seems very difficult to obtain an independent means of sampling such drops to check any radar inferences. We shall adopt a different approach, and test various forms of

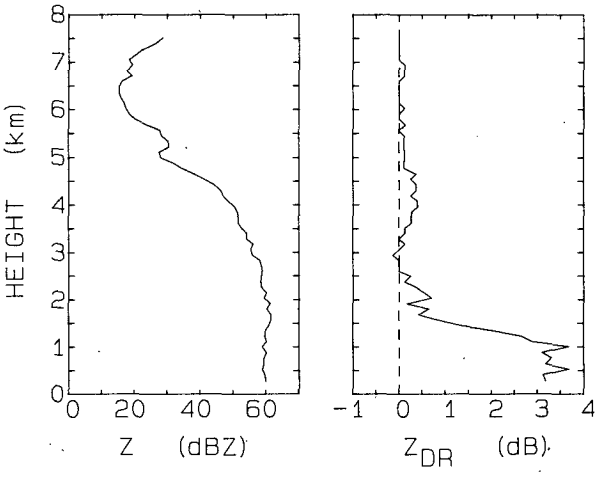

FIG. 3. A typical vertical profile through a vigorous convective cloud showing the monotonic increase in Z_{DR} as the ice particles fall through the freezing level at 3 km and subsequently melt.

TABLE 2. The average values of differential reflectivity for each 2 dBZ step in Z observed in heavy rain by the Chilbolton radar. The left-hand half of the table displays the mean, standard deviations (σ), skewness and kurtosis of the distributions of Z_{DR}—see Fig. 6 for the equivalent histograms. The right-hand side shows the equivalent parameters for log(Z_{DR})—see Fig. 7 for the histograms.

	Linear				Log			
Z (dBZ)	Z_{DR} (dB)	σ	Skewness	Kurtosis	logZ_{DR}	σ	Skewness	Kurtosis
30–32	0.86	0.70	2.15	10.5	−0.17	0.31	−0.05	2.99
32–34	0.96	0.70	2.15	8.07	−0.11	0.30	−0.14	2.93
34–36	1.06	0.75	1.70	6.77	−0.07	0.29	−0.04	2.78
36–38	1.17	0.71	1.60	6.39	0.00	0.25	+0.06	2.84
38–40	1.31	0.72	1.50	5.80	0.06	0.22	+0.13	2.90
40–42	1.48	0.74	1.42	5.16	0.12	0.20	+0.25	2.68
42–44	1.65	0.75	1.35	4.87	0.18	0.18	+0.27	2.95
44–46	1.79	0.73	1.26	4.81	0.22	0.16	+0.27	3.20
46–48	2.01	0.75	0.98	3.80	0.27	0.16	+0.15	2.28
48–50	2.23	0.74	0.83	3.52	0.33	0.14	+0.07	2.60
50–52	2.48	0.76	0.86	3.59	0.37	0.13	0.09	2.45
52–54	2.81	0.83	0.92	4.10	0.43	0.12	0.17	2.89
54–56	3.10	0.87	0.70	3.33	0.47	0.12	0.06	2.41
56–58	3.45	0.92	0.23	2.34	0.52	0.12	−0.28	2.41
58–60	3.73	0.96	0.11	2.46	0.56	0.11	−0.41	2.41
60–62	3.88	0.91	−0.07	—	0.58	0.11	−0.52	—
62–64	4.41	0.67	−0.44	—	0.64	0.07	−0.58	—

the raindrop size distribution to see which agrees most closely with the radar data. To compute the curves in Fig. 1, we assumed a D_{max} of 8 mm, a constant N_0 of 8000 m^{-3} mm^{-1}, and allowed D_0 to vary. We shall also explore the effect of fitting the data to a gamma distribution (Ulbrich and Atlas 1984):

$$N(D) = N_0 D^m \exp(-(3.67 + m)D/D_0). \quad (3)$$

The third parameter, m, reflects the breadth of the size distribution. The use of simplified size distributions is partially justified by the averaging of microscale features by the radar compared to disdrometer distributions.

Let us first consider the effect of truncating the exponential distribution. Both Joss and Waldwogel (1969) and Sachidananda and Zrnić (1987) used a maximum value of 6 mm but, in view of the above discussion, larger values such as the 9 mm used in the Z_{DR} calculations of Goddard and Cherry (1984) should be more realistic. Drops of 9 mm are stable in a low turbulence wind tunnel (Pruppacher and Beard 1970) and so, in the absence of collisions with other raindrops, it is reasonable to suppose they would exist in natural clouds. In Fig. 4 values of Z and Z_{DR} are plotted for maximum drop sizes of 8 and 10 mm, with the value of N_0 kept at 8000 m^{-3} mm^{-1} throughout. The agreement of the predictions using the 10 mm diameter cutoff with the average radar data is remarkable.

Figure 4 also explores the effect of the value of m in the gamma function. When $m = 0$ the gamma function reduces to the simple exponential, but some measurements indicate that natural raindrop spectra contain fewer of both the very large drops and the very small drops than would be the case for an exponential, and that a value of $m = 2$ is more appropriate (Ulbrich 1983). Again N_0 is kept constant at 8000 m^{-3} mm^{-1}, and the values for $D_{max} = 8$ and 10 mm with $m = 2$ are also plotted in Fig. 4. The agreement with observation is not as good; the lower predicted values of Z_{DR} at high rain rates reflect the lower concentrations of the large raindrops in the narrower spectrum.

If four variables are used in the raindrop spectrum then, for only two observables, an infinite combination

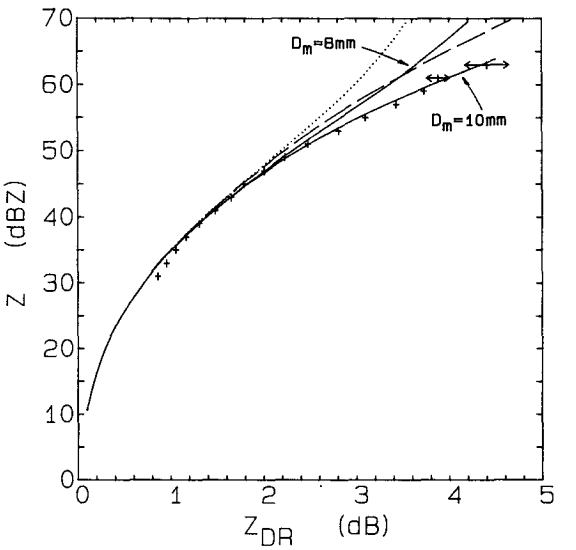

FIG. 4. The relationship of Z to Z_{DR} for variations in the parameters of the gamma drop size distribution. The solid lines are $m = 0$, $D_{max} = 8$ mm and $D_{max} = 10$ mm. The dotted line is $m = 2$, $D_{max} = 8$ mm and the dashed line is $m = 2$, $D_{max} = 10$ mm. The Beard and Chuang drop shapes were used and $N_0 = 8000$ m^{-3} mm^{-1}. The crosses are averaged Chilbolton data as in Fig. 1.

TABLE 3. Coefficients for the approximating polynomials. Coefficients are listed for an exponential drop size distribution with both 8 mm and 10 mm diameter truncation limits.

D_{max}	a_0	a_1	a_2	a_3	a_4	
(a) $Z = \sum_i a_i Z_{DR}^i$ for $N_0 = 8000$ m^{-3} mm^{-1} (Z and Z_{DR} in units of dB)						
8 and 10	2.620	95.14	−162.8	159.0	−59.15	0.1 dB ≤ Z_{DR} < 1.0 dB
8	17.38	21.28	−4.311	0.5259	−6.070E−4	1.0 dB ≤ Z_{DR} ≤ 4.5 dB
10	16.58	22.64	−5.020	0.6882	−0.03818	1.0 dB ≤ Z_{DR} ≤ 4.5 dB
(b) $D_0 = \sum_i a_i Z_{DR}^i$ (Z_{DR} in units of dB and D_0 in units of mm)						
8 and 10	0.4453	1.311	−0.9074	0.3863		0.1 dB ≤ Z_{DR} < 1.0 dB
8	0.04841	1.631	−0.5631	0.09509		1.0 dB ≤ Z_{DR} ≤ 4.5 dB
10	0.5998	0.6762	−0.04640	3.804E−3		1.0 dB ≤ Z_{DR} ≤ 4.5 dB
(c) $Z = \sum_i a_i Z_{DR}^i$ for $R = 1$ mm h^{-1} (Z and Z_{DR} in units of dB)						
8 and 10	17.86	20.57	−18.81	7.905		0.1 dB ≤ Z_{DR} < 1.0 dB
8	22.07	6.215	−0.8551	0.09013		1.0 dB ≤ Z_{DR} ≤ 4.5 dB
10	21.79	6.586	−0.9443	0.07051		1.0 dB ≤ Z_{DR} ≤ 4.5 dB

of values is possible. There is no reason, per se, to believe that the analytic form of the raindrop distribution should be the same for all rain rates; for example, N_0 can be adjusted to give the required value of Z for any value of Z_{DR}. In the absence of any other radar observable parameters, the most sensible choice for summertime convective clouds in the United Kingdom seems to be a pure exponential with a variable D_0, but keeping N_0 at 8000 m^{-3} mm^{-1} and D_{max} = 8 or 10 mm. A polynomial which fits these theoretical computations and gives Z correct to 0.2 dBZ is given in Table 3.

Figure 5 compares the predicted values of Z_{DR} as a function of D_0 for a pure exponential raindrop spectrum. The polynomials which fit the curves for the Beard and Chuang shapes to an accuracy of 0.05 mm in D_0 are given in Table 3. For comparison purposes we also plot the relationship ($Z_{DR} = 0.45 D_0^{1.56}$) suggested by Seliga et al. (1986) for Green's (1975) shapes. Because this equation is constrained to pass through the origin and can have no points of inflection, it cannot represent the dependence very accurately.

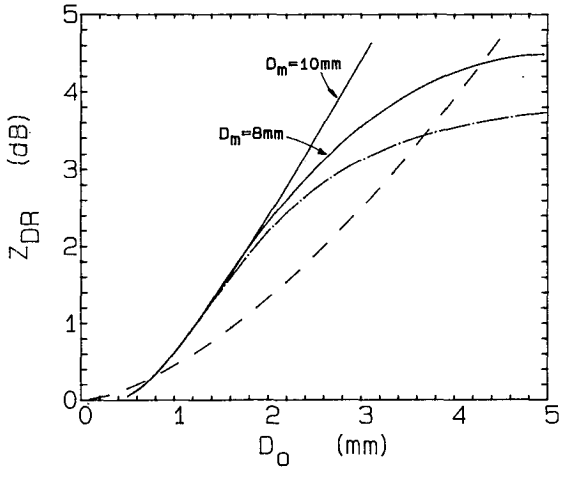

FIG. 5. A comparison of the various proposed relationships between Z_{DR} and D_0. Solid line: Beard and Chuang drop shapes for D_{max} = 8 and 10 mm. Dash–dot line: Pruppacher and Pitter shapes for D_{max} = 8 mm. Dashed line: $Z_{DR} = 0.45 D_0^{1.56}$ (Seliga et al. 1986).

So far we have used the values of Z_{DR} computed at 0°C. Some values at +10°C and −10°C are presented in Table 1. Although these computations are not complete, and the change in Z_{DR} for the full Mie–Gans theory is not a simple function of temperature, the values in Table 1 indicate that there would only be a small change in the curves in Fig. 1 over this temperature range. The values at −10°C are of interest when interpreting transient narrow columns of positive Z_{DR} which extend up to 2 km above the freezing level in vigorous convection. We have argued (Illingworth et al. 1987) that these are due to supercooled rain drops.

These effects of temperature at S band (10 cm) should be small, but seem to be more serious at C band (5.5 cm). Computations at 5.5 cm wavelength, but using the Pruppacher and Pitter drop shapes (Meischner et al. 1988), show a pronounced resonance for 6 mm drops with a maximum Z_{DR} of nearly 8 dB at 20°C, falling to 4 dB for 7 and 8 mm. The maximum is much less marked at 0°C. The use of the Beard and Chuang shapes will modify these values, but they indicate that severe problems could arise in any quantitative analysis of high Z_{DR} regions observed at C-band.

3. Variability of natural raindrop spectra

In the previous section we concentrated upon obtaining average values of Z_{DR} for a given magnitude

of Z. Particular observations of Z and Z_{DR} do not, of course, lie on this average curve; this enables Z_{DR} to be used as an independent observable. The curve in Fig. 1 for the Beard and Chuang drop shapes represents the best available estimate of the values of Z and Z_{DR} for a value of $N_0 = 8000\ m^{-3}\ mm^{-1}$ in the exponential raindrop size spectrum of Eq. (2). For any particular observation of Z and Z_{DR}, the value of D_0 can be derived from Z_{DR}, and N_0 found from Fig. 1, using the fact that Z scales linearly with N_0.

Histograms of the frequency of occurrence of different values of Z_{DR} for each interval of 2 dBZ in Z are plotted in Fig. 6. The mean values of Z_{DR} of each histogram are those plotted in Fig. 1. The width of the histograms can be used to estimate the variability of naturally occurring raindrop spectra. Histograms for values of Z less than 30 dBZ are not presented because the resolution of Z_{DR} obtainable by the radar is insufficient; histograms for Z above 60 dBZ are not shown because the sample sizes are too small. An asymmetry of the distributions in Fig. 6 is evident, with a long tail showing that values of Z_{DR} many times the mean occasionally occur. This implies that values of N_0 are generally close to $8000\ m^{-3}\ mm^{-1}$, but that on occasion much lower values occur. Figure 4 shows that nonexponential drop size spectra such as gamma functions will also contribute to the observed variability, but that the long tail in Z_{DR} cannot be explained without invoking low drop concentrations. We have drawn attention (Illingworth et al. 1987) to the anomalously high values of Z_{DR} observed in some isolated first echoes, but, because of their limited spatial extent, such data are not included in the "average" data. The unusual characteristics of these first echoes may be reemphasized with reference to Fig. 6. In these isolated clouds Z values of 30 and 40 dBZ were accompanied by Z_{DR} values of 3 and 4 dB, respectively; the statistical analysis presented in Fig. 6 shows that for these two values of Z, 98% of the data in the sample were accompanied by Z_{DR} values of a lower magnitude.

In view of the skewness of the Z_{DR} histograms in Fig. 6, the histograms were recomputed for $\log(Z_{DR})$. The results are displayed in Fig. 7 and a greater symmetry of the distributions is apparent. This is confirmed by Table 2, which provides the values of standard deviations, skewness and kurtosis for the histograms in Figs. 6 and 7. The skewness (defined as the ratio of the third moment to the cube of the standard deviation) of the $\log(Z_{DR})$ distributions is about one tenth that for the linear Z_{DR} histograms for the range of Z from 30 to 50 dBZ; above 50 dBZ the difference is less clear, but this may be affected by the smallness of the sample size. The kurtosis (the ratio of the fourth moment to the fourth power of the standard deviation) should be 3 for a normal distribution; higher values arise if the wings of the distribution are wider than for a normal distribution. Again, the values of kurtosis for the $\log(Z_{DR})$ histograms in the Z range 30–50 dBZ are close to 3, whereas the linear Z_{DR} histograms have much greater values. Kurtosis values for Z above 60 dBZ are not meaningful because of the small sample size. The data in Table 2 are for clouds on many dif-

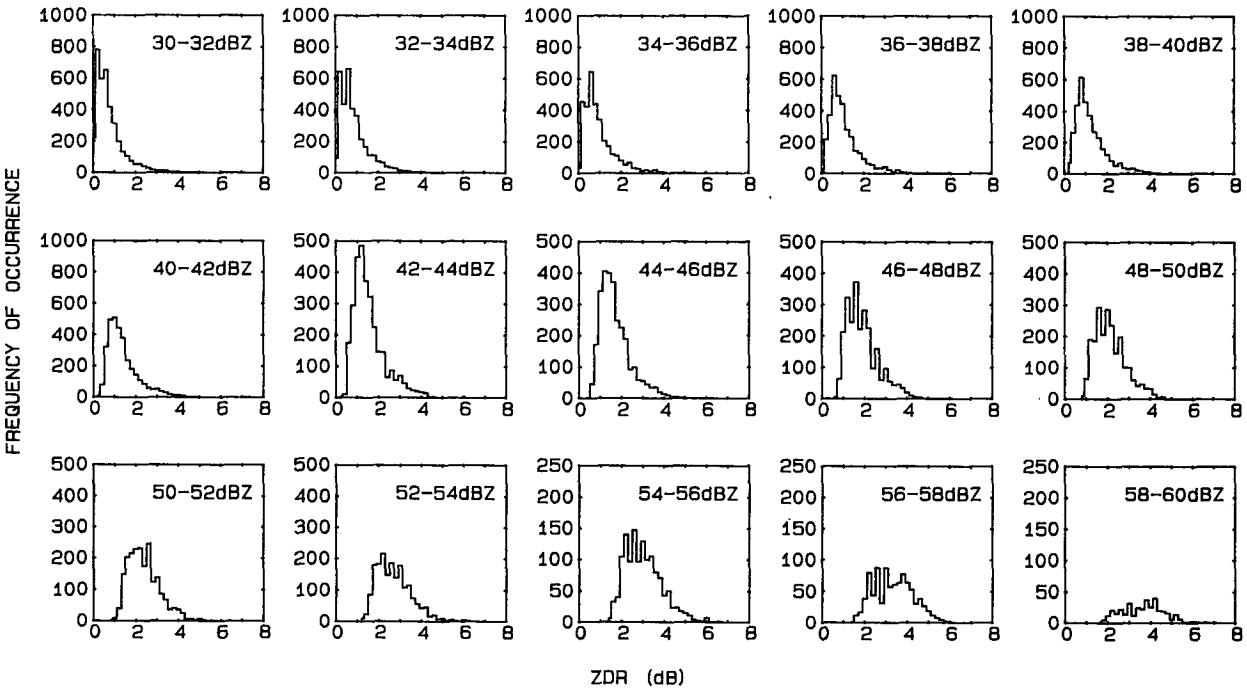

FIG. 6. Histograms of the number of Z_{DR} values associated with 2 dB intervals in Z. The data were observed for summer convective clouds in 1983 and 1984. The number in the corner of each histogram indicates the centre of the particular Z interval in units of dBZ.

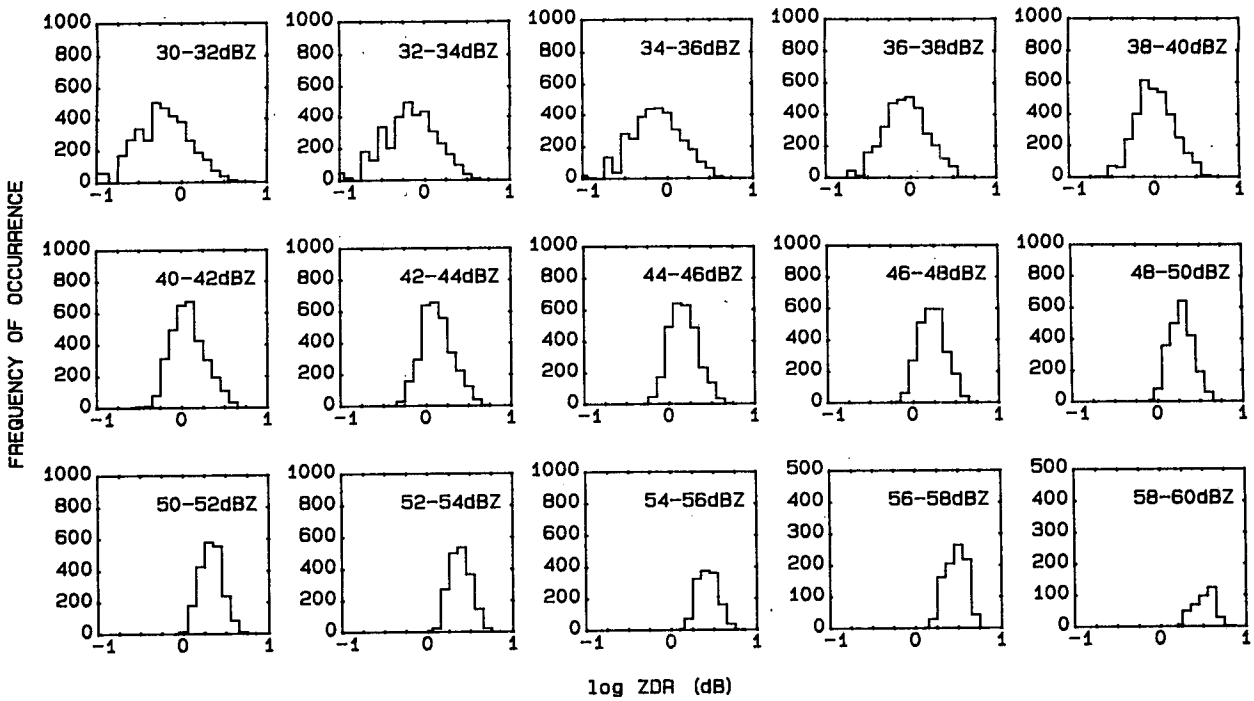

FIG. 7. The histograms of Fig. 4 replotted with logarithmic spaced Z_{DR} bins.

ferent days. No systematic differences were apparent when the observations of individual clouds were considered.

The statistics in Table 2 of the variability of spectra may be of use in interpreting conventional radar data and for statistical studies of problems related to electromagnetic propagation in the lower troposphere.

4. The variability of radar derived rainfall rates

a. Derivation of rain rate

In this section we compare various proposed relationships for deriving rainfall rates when both Z and Z_{DR} are available. Figure 8 compares the values of rain rate (R) as a function of Z and Z_{DR} using the original shapes of Pruppacher and Pitter and the new shapes of Beard and Chuang for an exponential size distribution. For a given Z_{DR} the values of R scale linearly with Z. On the figure, curves for 10 and 100 mm h^{-1} are plotted. The new drop shapes lead to slightly lower rainfall rates for a given Z/Z_{DR} combination; for example, for a Z_{DR} of 3 and 3.7 dB the reductions are 26% and 44%, respectively. The effect of using a D_{max} of 10 mm is marked with the dashed line; this uncertainty over choice of truncation limit only becomes significant for Z_{DR} above 3 dB, at 4 dB the reduction in deduced rain rate is about 25%.

An analytic approximation to the theoretical curves in Fig. 8 for a rain rate of 1 mm h^{-1} using the Beard and Chuang shapes modified for small drops, is given in Table 3c. Measurement errors in Z_{DR} affect the precision with which rain rates may be estimated. Because of the changing gradient of the curves in Fig. 8, the errors in the rainfall estimate will increase for lower values of Z_{DR}. When Z_{DR} is zero it provides only an upper bound on the mean drop size, and so, for a given Z, the Z_{DR} information merely sets a lower limit on the rainfall rate. The data presented from the Chilbolton radar in this paper have a standard error of about 0.1 dB in Z_{DR}.

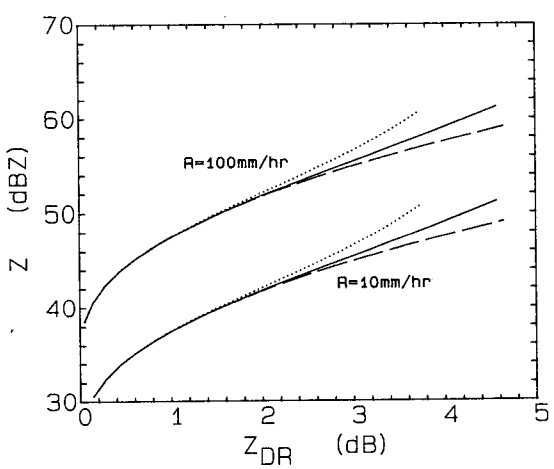

FIG. 8. The variation of Z with Z_{DR} expected for constant rainfall rates. The lower set of curves is for a rainfall rate of 10 mm h^{-1} and the upper set is for a rate of 100 mm h^{-1}. The solid line is the Beard and Chuang drop shapes and an exponential drop size distribution with D_{max} = 8 mm, while the dashed line is for the D_{max} = 10 mm. The dotted line shows the rainfall expected with the Pruppacher and Pitter shapes for an exponential distribution with D_{max} = 8 mm.

Several other theoretical relationships have been published recently that relate the rainfall rate to the observed values of Z and Z_{DR} and these are compared in Fig. 9. The curves are for a rain rate of 1 mm h^{-1}, and, as in Fig. 8, the rain rates scale linearly with Z. Seliga et al. [1986, Eq. (35)] use Green's (1975) drop shapes and suggest for Z_{DR} in dB:

$$Z\,(\mathrm{dBZ}) = 27.10 + 10.40 \log(Z_{DR}), \qquad 0.2 < Z_{DR} < 0.7 \quad (4a)$$

$$Z\,(\mathrm{dBZ}) = 27.98 + 16.70 \log(Z_{DR}), \qquad 0.7 < Z_{DR} < 2.6. \quad (4b)$$

Because we now believe that small drops are slightly more spherical than Green's formula, Eq. (4) overestimates the rainfall by about 1.5 dB (40%) for low values of Z_{DR}, and conversely, for large values of Z_{DR} the Green shapes are insufficiently oblate and the rain rate is underestimated by about 1.5 dB (30%). Seliga et al. analyze the drop size distributions measured during a 3 hour heavy rainfall event. They compute the theoretical values of Z and Z_{DR}, which would have been observed, and show that using the two observables, Z and Z_{DR}, should give a better estimate of rainfall rate than an empirical Z–R relationship. This argument demonstrates the validity of the technique but does not prove that the drop shapes used for Eq. 4 are correct.

The Z and Z_{DR} radar data for part of a single 15 km × 15 km PPI scan were analyzed by Sachidanada and Zrnić (1987). The data were compared with the theoretical relationship for an exponential drop size distribution with a maximum size of 6 mm using Green's (1975) drop shapes. For a rain rate of 1 mm h^{-1} their Eq. (8) with Z_{DR} in dB may be expressed as

$$Z\,(\mathrm{dBZ}) = 21.65 + 4.86 Z_{DR}. \quad (5)$$

They claim that this linear relationship fitted the theoretical curve to within 3%, or 0.05 dB; in view of the other theoretical curves in Fig. 9, this seems difficult to understand. They comment that the scatter of the observations of Z and Z_{DR} for the single PPI scan seem large when compared with the scatter simulated by generating random values for the drop size distribution parameters in the ranges:

$$30 < N_0 < 30\,000 \quad [\mathrm{mm}^{-1}\ \mathrm{m}^{-3}]$$

$$-2 < m < +3$$

$$4 < D_{\max} < 6 \quad [\mathrm{mm}]$$

$$0.27 < D_0 < 1.23 \quad [\mathrm{mm}].$$

Accordingly, the observations from one part of the scan that seemed to have a particularly high scatter were discounted, although we note that the highest values of D_0 used in the simulation is equivalent to a rain rate of only 6 mm h^{-1} for Marshall–Palmer rain. Noticing that the mean value of Z for a given Z_{DR} for the remaining data seemed higher than expected, they suggested that the raindrops were very oblate and proposed a relationship between the axial ratio and drop diameter (D):

$$a/b = 1 - 0.64 D^{1.25}. \quad (6)$$

A slight dip in the mean values of Z for higher values of Z_{DR} was interpreted in terms of drop breakup. For the more oblate shapes they suggested a revised relationship for R = 1 mm h^{-1}:

$$Z = 22.39 + 3.49 Z_{DR}. \quad (7)$$

Our experience with the Chilbolton data is that the averages from a single PPI are highly variable and that such generalizations embodied in Eqs. (6) and (7) are not justified.

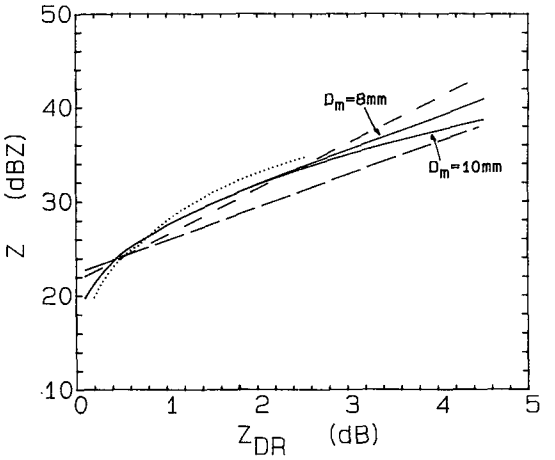

FIG. 9. A comparison of various suggested relationships for deriving rainfall rates from Z and Z_{DR}. The curves are for rain rates of 1 mm h^{-1}. Solid lines: This study using the modified Beard and Chuang shapes. Dotted line: Seliga et al. (1986), Green's shapes, Eq. 4. Dashed lines: Sachidananda and Zrnić (1987), Green's shapes, Short dashes—Eq. (5); Long dashes—Eq. 7.

b. *Variability of rain rates for a given Z*

In order to obtain an estimate of the variability of natural rainfall for a given Z, the histograms of Chilbolton data for Z_{DR} in Fig. 6 have been replotted in Fig. 10. The polynomial in Table 3c has been used to convert the values of Z_{DR} to a rainfall rate. The data are summarized in Table 4, where, for a given Z, the mean rain rate and its standard deviation are presented. We note that the standard deviation of the inferred rain rate is somewhat greater than half the mean rate, but that the distributions are skewed so that, on occasion, the inferred rain rate is many times that expected from a simple Z–R relationship. The data is taken with a sample volume that is typically a 300 m cube; if this volume was increased then averaging would be expected to narrow the histograms in Fig. 10.

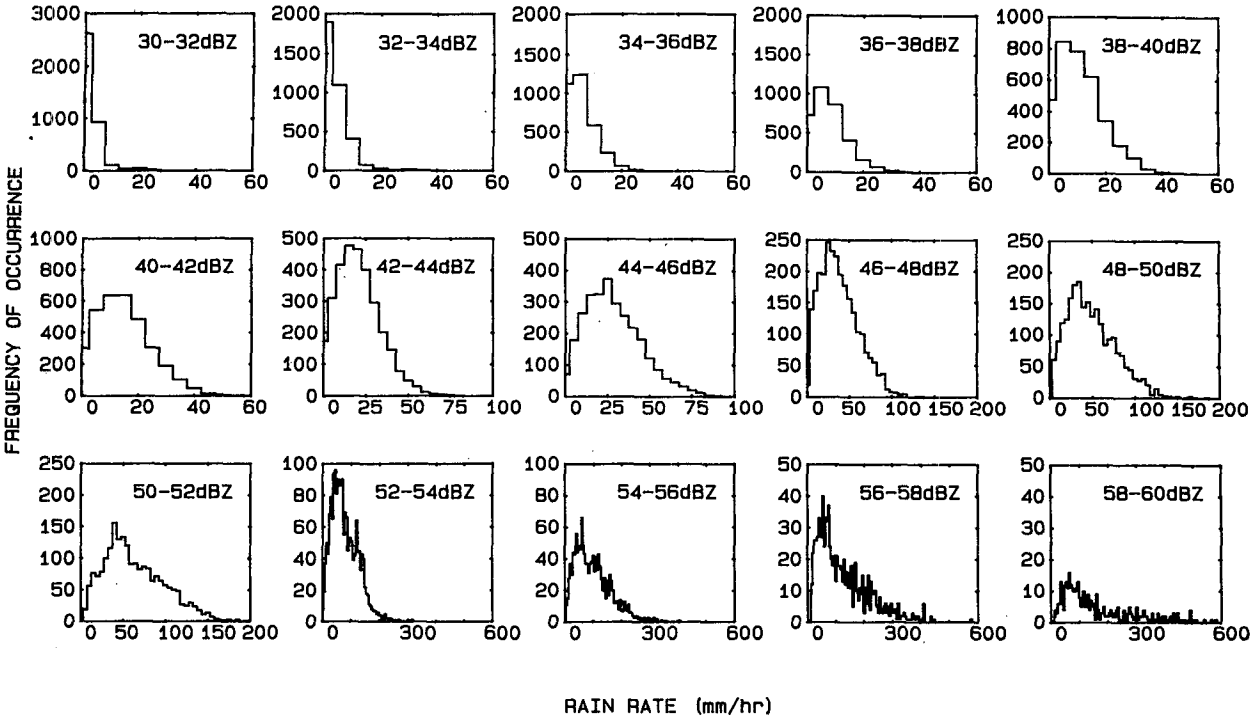

FIG. 10. Histograms of the rainfall rates associated with 2 dB intervals in Z. The data are from Fig. 4, using Table 3 to compute the rainfall rate from Z and Z_{DR}.

Before applying the relationships in Table 2 the accuracy of the observations must be considered. The Chilbolton radar estimates Z_{DR} to an accuracy of about 0.1 dB, introducing an error in rain rates of about 12% (that is, 0.5 dB) for values of Z_{DR} above 1 dB (Fig. 9). When Z_{DR} values approaching zero are common, as is the case in Table 4 when Z is below 40 dBZ, then the errors in the derived rainfall rate are larger.

The fundamental accuracy limiting the Z_{DR} measurement should be analyzed before calculating rainfall rates. Even if we assume that there are no instrumental errors due to mismatch of the channels for horizontal and vertical polarization and that the beam is filled with rainfall with no severe reflectivity gradients across the sample volume, the accuracy of the Z_{DR} estimate is limited by the finite dwell time of the radar. Bringi et al. (1983) show that about 40–60 independent sample pairs of Z_H and Z_V are required if Z_{DR} is to be measured with a standard error as low as 0.1 dB. The time to independence is related to the width of the Doppler spectrum of the target and is usually in the range 20 to 40 ms at 10 cm wavelength. The Chilbolton Z_{DR} data are obtained with a time integration of 210 ms and spatial integration over four 75 m range gates. If faster scanning is employed with no spatial averaging then the number of independent samples will fall. If the number of samples is only six, for example, the standard error in Z_{DR} will be about 0.5 dB. Even for large values of Z_{DR} this would lead to an error of nearly 100% in the derived rain rate.

TABLE 4. The average values of radar-inferred rainfall rate (R) for each 2 dBZ step in Z, observed in heavy rain by the Chilbolton radar. Histograms of the data are shown in Fig. 10; σ_R is the standard deviation and n the sample size.

Z (dBZ)	R (mm h^{-1})	σ_R (mm h^{-1})	n
31.0	4.41	3.94	3760
33.0	5.83	4.73	3520
35.0	7.96	5.88	3311
37.0	10.30	6.60	3347
39.0	13.50	8.10	3391
41.0	17.40	9.90	3285
43.0	23.10	13.00	3067
45.0	31.00	17.00	2871
47.0	40.50	22.70	2586
49.0	52.00	28.80	2263
51.0	66.20	35.90	2090
53.0	80.80	46.50	1871
55.0	102.00	64.00	1346
57.0	127.00	92.00	922
59.0	162.00	130.00	376

5. Discussion and conclusions

The precise shape of raindrops which should be used for the interpretation of Z_{DR} measurements has been a matter of considerable debate. The radar results reported in this paper are in good agreement with the new, more accurate, shapes proposed for the large drops by Beard and Chuang (1987) and the Goddard et al. (1983) shapes for drops below 3 mm. In the absence of any third observable reflecting the value of m in the

gamma distribution, the most reasonable spectrum for interpreting the Z and Z_{DR} observations is the exponential of Eq. (2) with a D_{max} = 8 mm. In heavy rain with Z values above 50 dBZ there is an indication that a D_{max} = 10 mm could be used.

Based upon these new drop shapes and for an exponential distribution of raindrop sizes, the analytic expressions in Table 3 appear most appropriate for calculating D_0 from the observed value of Z_{DR} and for deriving N_0 and the rainfall rate from Z and Z_{DR} data. Particular attention should be paid to errors introduced into Z_{DR} by sampling limitations.

In Illingworth et al. (1987) it was argued that values of Z_{DR} of 6 dB were due to a monodispersed distribution of large raindrops, and the new drop shapes discussed in this paper support their interpretation. From a radar analysis, Caylor and Illingworth (1986) hypothesized that large raindrops must be more oblate than was commonly accepted; the more oblate shapes have now been confirmed independently, and give more consistent agreement with the radar data. The extreme oblateness of the very large drops proposed by Caylor and Illingworth (1986) are too exaggerated, however, and those of Beard and Chuang (1987) should be used.

Acknowledgments. This research was supported by the Meteorological Office, by NERC Grant GR3/5896 and by AFOSR-88-0121. We are indebted to Dr. Holt of the Department of Mathematics, Essex University for the Mie–Gans calculations in Table 1. Computing facilities were provided by the SERC under GR/D69372. One of us (IJC) acknowledges the assistance of an ORS studentship. We thank our colleagues S. M. Cherry and J. W. F. Goddard for supplying the Chilbolton data and for numerous enlightening discussions.

REFERENCES

Beard, K. V., D. B. Johnson and D. Baumgardner, 1986: Aircraft observations of large raindrops in warm, shallow, convective clouds. *Geophys. Res. Lett.*, **13,** 991–994.

Beard, K. V., 1976: Terminal velocity and shape of cloud and precipitation drops aloft. *J. Atmos. Sci.*, **34,** 851–864.

——, and D. Chuang, 1987: A new model for the equilibrium shape of raindrops. *J. Atmos. Sci.*, **44,** 1509–1524.

——, and H. T. Ochs, 1988: Wake-excited raindrop oscillations. Preprints, *Tenth Inter. Cloud Physics Conf.*, Deutscher Wetterdienst, Offenbach-am-Main, 7–8.

Bringi, V. N., T. A. Seliga and S. M. Cherry, 1983: Statistical properties of the dual-polarization differential reflectivity (Z_{DR}) radar signal. *IEEE Trans. Geo. Remote. Sens.*, **GE-21,** 215–220.

Caylor, I. J., and A. J. Illingworth, 1986: Observations of the growth and evolution of raindrops using dual-polarization radar. Preprints, *22nd Conf. Radar Meteorology,* Snowmass, Amer. Meteor. Soc., 88–91.

Chandrasekar, V., W. A. Cooper and V. N. Bringi, 1988: Axis ratios and oscillations of raindrops. *J. Atmos. Sci.*, **45,** 1323–1333.

Cherry, S. M., and J. W. F. Goddard, 1982: Design features of dual polarisation radar. *URSI Open Symposium on Multiple Parameter Radar Measurements of Precipitation,* Bournemouth, U.K.

Cooper, W. A., V. N. Bringi, V. Chandrasekar and T. A. Seliga, 1983: Analysis of raindrop parameters using a 2D precipitation probe with application to differential reflectivity. Preprints, *21st Conf. Radar Meteorology,* Edmonton, Amer. Meteor. Soc., 448–493.

Doviak, R. J., and D. S. Zrnić, 1984: *Doppler Radar and Weather Observation.* Academic Press, 458 pp.

Goddard, J. W. F., and S. M. Cherry, 1984: The ability of dual polarisation radar (copolar linear) to predict rainfall rate and microwave attenuation. *Radio Sci.*, **19,** 201–208.

——, —— and V. N. Bringi, 1983: Comparisons of dual-polarization radar measurements of rain with ground-based distrometer measurements. *J. Appl. Meteor.*, **21,** 252–256.

Green, A. W., 1975: An approximation for the shape of large raindrops. *J. Appl. Meteor.*, **14,** 1578–1583.

Hall, M. P. M., J. W. F. Goddard and S. M. Cherry, 1984: Identification of hydrometeors and other targets by dual-polarisation radar. *Radio Sci.*, **19,** 132–140.

Illingworth, A. J., J. W. F. Goddard and S. M. Cherry, 1986: Detection of hail by dual-polarization radar. *Nature,* **320,** 431–433.

——, —— and ——, 1987: Polarization radar studies of precipitation development in convective storms. *Quart. J. Roy. Meteor. Soc.*, **113,** 469–489.

Joss, J., and A. Waldvogel, 1967: A raindrop spectrometer with automatic readout. *Pure Appl. Geophys.*, **68,** 240–246.

——, and ——, 1969: Raindrop size distribution and sampling size errors. *J. Atmos. Sci.*, **26,** 566–569.

Marshall, J. S., and W. M. K. Palmer, 1948: The distribution of raindrops with size. *J. Meteor.*, **5,** 165–166.

Meischner, P., V. N. Bringi and T. Jank, 1988: Multiparameter Doppler radar observations of a squall line with the polarimetric DFVLR radar. Preprints, *Tenth Int. Cloud Physics Conf.*, Deutscher Wetterdienst, Offenbach-am-Main, 330–332.

Pruppacher, H. R., and K. V. Beard, 1970: A wind tunnel investigation of the internal circulation and shape of water drops falling at terminal velocity in air. *Quart. J. Roy. Meteor. Soc.*, **96,** 247–256.

——, and R. L. Pitter, 1971: A semi-empirical determination of the shape of cloud and rain drops. *J. Atmos. Sci.*, **28,** 86–94.

Rasmussen, R. M., V. Levizzani and H. Pruppacher, 1984: A wind tunnel and theoretical study of the melting behaviour of atmospheric ice particles: Part III: Experiment and theory for spherical ice particles of radius above 500 um. *J. Atmos. Sci.*, **41,** 381–388.

——, C. Walcek, H. R. Pruppacher, S. K. Mitra, J. Lew, V. Levizzani, P. K. Wang and U. Barth, 1985: A wind tunnel investigation of the effect of an external vertical electric field on the shape of electrically uncharged rain drops. *J. Atmos. Sci.*, **42,** 1647–1652.

Sachidananda, M., and D. S. Zrnić, 1987: Rain rate estimates from differential polarization measurements. *J. Atmos. Oceanic Technol.*, **4,** 588–598.

Seliga, T. A., and V. N. Bringi, 1976: Potential use of radar differential reflectivity measurements at orthogonal polarizations for measuring precipitation. *J. Appl. Meteor.*, **15,** 69–76.

——, K. Aydin and H. Direskeneli, 1986: Disdrometer measurements during an intense rainfall event in central Illinois: Implications for differential reflectivity radar observations. *J. Climate Appl. Meteor.*, **25,** 835–846.

Ulbrich, C. W., 1983: Natural variations in the analytical form of the raindrop size distribution. *J. Climate Appl. Meteor.*, **22,** 1764–1775.

——, and D. Atlas, 1984: Assessment of the contribution of differential polarization to improved rainfall measurements. *Radio Sci.*, **19,** 49–57.

Willis, P. T., 1984: Functional fits to some observed drop size distributions and parameterization of rain. *J. Atmos. Sci.*, **41,** 1648–1661.

Wilson, J. W., and E. A. Brandes, 1979: Radar measurements of rainfall—a summary. *Bull. Amer. Meteor. Soc.*, **60,** 1048–1058.